A High Q 2D-Length Extension Mode Resonator for potential Time-Frequency applications

P. Chapellier, P. Lavenus
Sensors and Microtechnology unit
ONERA
Châtillon, France

B. Dulmet
FEMTO-ST, UMR CNRS 6174
Besançon, France

***Abstract*—In this paper, high quality factor two dimensional length-extension mode (2D-LEM) quartz resonator showing promising performances for Time & Frequency (T&F) applications are reported. They combine the intrinsic qualities of quartz (high Q, low temperature sensitivity and piezoelectricity) and the advantages of silicon resonators: small dimensions, low power consumption and collective processes. Several processes have been investigated as well as several sizes and designs of resonators. A high quality factor (Q), exceeding 200 000, two dimensional length-extension mode (2D-LEM) quartz resonator vibrating at 2.2 and 3 MHz**

Keywords—Quartz resonator; DRIE; Time & Frequency; MEMS oscillator.

I. INTRODUCTION

A three dimensional Length-Extension Mode (3D-LEM) quartz resonator were designed and developed in previous work [1] in order to reach quantum ground state. It successfully exhibited a very high Q of 2 000 000 at 4.0 MHz, reaching a Q.f product of 8.10^{12} near the theoretical limit of quartz of $3.2.10^{13}$ due to Akiezher losses [2]. This LEM resonator design could be a potential candidate for time & frequency applications.

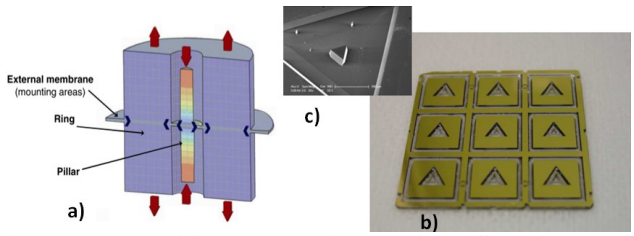

Fig. 1. a) Concept of the 3D-LEM: a ring around the pillar with an out of phase length-extension vibration, b) 1.5-inches square quartz wafer including 9 3D-LEM made using wet etching, c) detail of the micro-pillar.

Unfortunately, the resonator is quite bulky (1x1x0.5 cm^3) and its 3D design does not allow electrical actuation. To overcome these issues, compact planar two dimensional length-extension mode (2D-LEM) resonators using similar working principle have been developed. In this paper, two types of 2D-LEM resonators , denoted type I and type II, are studied.

II. RESONATORS DESIGN AND QUALITY FACTOR

A. Mode of interest

2D-LEM resonators of type I and II consist of a beam vibrating in extension-compression. The resonant frequency is around a few MHz with a central beam of few millimeters. More precisely, the fundamental mode (n=0) and harmonics [3] for Z-cut quartz are given by equation (1):

$$f_{2n+1} = (2n+1)\frac{2.72}{L}MHz \qquad (1)$$

where L is the total length of the vibrating beam in mm and n is the mode number. As seen from (1), the resonant frequency can be adjusted depending on the targeted applications by varying L. This should be done though homothetic transformations of the whole structure to maintain the optimized decoupling between the beam and the mounting area. For the ease of processing, resonators are actuated via gold electrodes only deposited on the upper surface. The electric field is generated along X-axis while the engendered beam displacement occurs along Y-axis as it can been seen in Fig. 2.

B. Resonators designs

1) First design, "type I" resonator

In addition to the central beam, the type I resonator has two large lateral beams that vibrate in an in-plane forced flexure movement that compensates for the shear stress induced though the Poisson effect by the vibrating central beam. Thus, the confinement of the stress close to the central beam allows

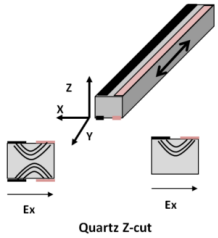

Fig. 2. Electrode scheme for the actuation of the extension mode of a Quartz Z-cut beam oriented along the Y axis.Ideally, the electrodes should be deposited on both face to optimize the electric field along X-. Real electrode system on the right.

minimized deformation in the mounting area, leading to a high intrinsic quality factor.

The deformation mode of the type I resonator obtained with Finite Element Method simulations (FEM) is shown in Fig. 3.

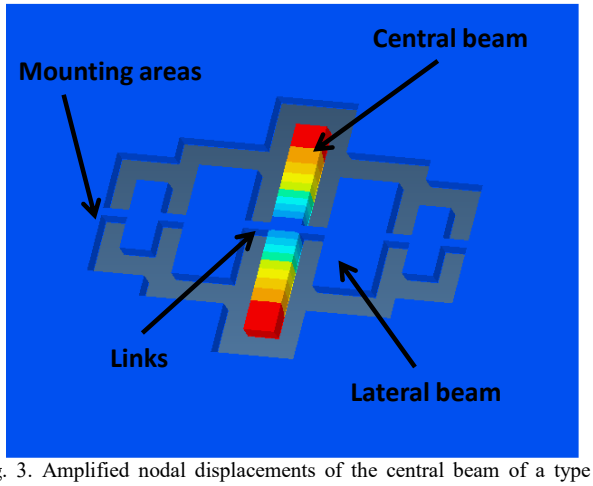

Fig. 3. Amplified nodal displacements of the central beam of a type I resonator during its length-extension mode vibration.

2) Second design, "type II" resonator

In addition to the central beam, the type II resonator has two thin lateral beams. The decoupling between the central beam and the mounting area is partly ensured by a flexure movement similar to the type I resonator. This is illustrated in Fig.4 (left) which shows the magnified deformation along X axis of the type II 2D-LEM resonator. The type II 2D-LEM resonator also benefits from an additional compensation mechanism relying on an length-extension vibration of the lateral beam in opposite phase in comparison to the central beam as shown in Fig.4 (right). This figure shows the magnified deformation along Y axis.

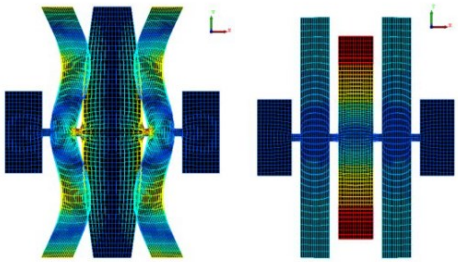

Fig. 4. Type II 2D-LEM resonator vibrating mode. On the left, the X component of the magnified deformation showing flexure movement in thelateral beams. On the right, the Y predominant extension out-of-phase component of the deformation of pillar and lateral beams.

C. Quality factor

The quality factor of a resonator can be defined as the ratio of the stored energy over the energy dissipated per cycle via different damping mechanisms. It can be written under vacuum as:

$$\frac{1}{Q} = \frac{1}{Q_{visc}} + \frac{1}{Q_{AKE}} + \frac{1}{Q_{TED}} + \frac{1}{Q_{anchor}}$$

where damping mecanisms are briefly described in Table I. In the 2D-LEM case, a more complete description can be found in [5]. From the FEM simulations a quality factor around 600 000 is expected for resonators vibrating at a few MHz making possible to reach a $Q.f$ product between 1,2 and $1{,}5.10^{12}$ Hz.

Table 1. Summary of the damping mecanims and estimations in the 2D-LEM case.

Notation	Damping source	Model and estimation in the 2D-LEM case
Q_{anchor}	Strain energy that leaks at the anchors (i.e. mounting areas)	Simulations using Finite Element Method (FEM) By design $Q_{anchor}>10^8$ for perfect geometry
Q_{TED}	Thermoeslatiscity damping is the energy loss due the bending of the resonator: creation of a thermal gradient where there is a strain gradient leading to thermal transport and damping.	$Q_{TED}>10^7$ in the case of the 2D-LEM because there is no flexion of the central pillar.
Q_{AKE}	Akhiezer loss is the quantic limit: the displacement induces a deformation of the lattice thus a return to thermodynamics with phonon-phonon interaction.	$Q.f$ depends on the material. For quartz, the limit is $3{,}2.10^{13}$ Hz. For a vibrating structure at few MHz, $Q_{AKE}\sim10^7$
Q_{visc}	Arises from the viscosity of the gold from the electrodes.	Analytical model has been developed in [6]. The model depends on the ratio of the vibrating thickness of quartz and gold as well as the resonant frequency. $Q_{visc}=6{,}1.10^5$ at 3 MHz and $5{,}7.10^5$ at 2.2 MHz

III. Process Flow

Standard wet etching using hydrofluoric acid (HF) is not suited for etching the vibrating part due to its high anisotropy and faceting [7]. Deep Reactive Ion Etching of quartz has been developed for the last decade thanks to the development of high density plasma etcher. Resonators using DRIE have been reported [8][9] but vertical etching quartz over several tens to hundred microns is still challenging. In the present study, two process flows has been used and compared.

A. Process 1: Two DRIE steps process

Process 1 is described in Fig. 5. and uses two DRIE steps: once the patterns of the resonators are made with the first

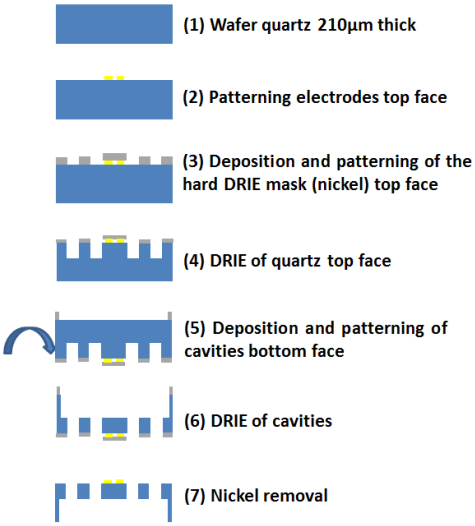

Fig. 5 Process flow 1 using two DRIE steps.

etching step, the wafer is flipped and cavities are etched until the desired thickness and full liberation of the structures.

This DRIE process uses a combination of a fluorocarbon gas (CF_4) and dioxygen: vertical etching of quartz takes place thanks to the presence of a passivating polymer [10] on the sidewall.

This process suffers from a major issue : the wafer is craking due to the release of the stress induced by DRIE heating as shown in the Fig. 6., This phenomon has been observed in previous work [8].

B. *Process 2: One DRIE step process with cavities etched by wet chemical solution*

To reduce the craking, a process with reduced duration of the DRIE steps has been tested and is presented in Fig. 7 : in this case, the cavities were etched with a wet chemical solution HF-NH_4F has been developed and . Chromium/Gold layers are evaporated on both faces as they serve as electrodes and etching mask during the wet chemical etching step. Only the back side of the vibrating part is rough as the release of the structure is made by the DRIE step.

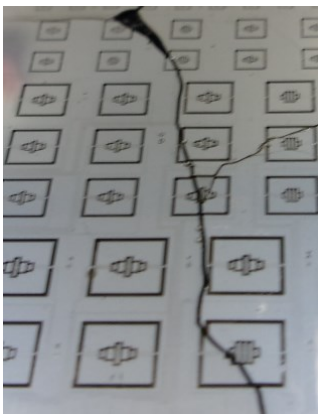

Fig. 6. Photography of an example of craking after DRIE step.

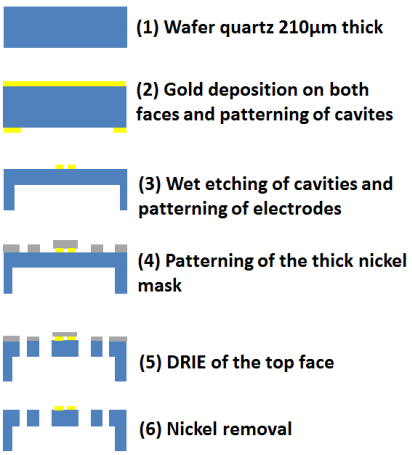

Fig. 7 Process flow 3 using wet etching to create cavities and one DRIE step on top face. Etching gas is the same as in process 2.

IV. Results & Discussion

A. *Results of process 1*

1) *Measurements*

Resonators vibrating at 3.0 and 2.2 MHz have been manufactured (Fig. 8) and electrical measurements were performed under vacuum (10^{-4} mbar) with impedance analyser (Keysight EA990A) and are given in table 2 with others works on similar devices. Fits are obtained with a standard Butterwoth-Van Dyke model (BVD). Simulated frequency, theoretical values and experimental values are in very good agreement.Experimental quality factors as high as 180 000 for type II resonators vibrating at 2.2 MHz was found but these are still half of the value that is expected from FEM simulations, meaning that one or more damping mechanism has been underestimated or wrongly neglected.

2) *Analysis of the measured quality factors*

One significant difference between the real structure and the simulated one lies in the sidewalls angle : DRIE leads to not perfectly vertical sidewalls as illustrated in Fig. 9. New FEM simulations have been carried out to estimate how this non verticality modify the losses in the mounting areas (Q_{anchor}).FEM simulations give us the dependency of the Q_{anchor} versus sidewall angle in Fig. 9. It appears that energy trapping

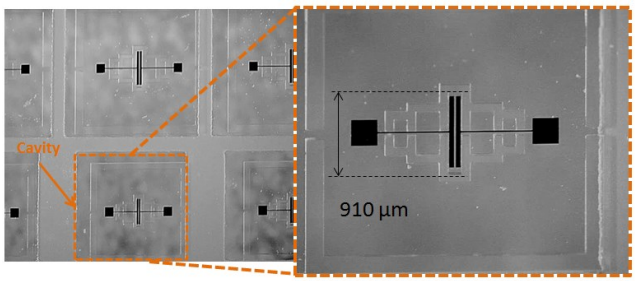

Fig. 8. Right, top line type I resonators vibrating at 2.2 MHz, bottom line at 3 MHz. Left, focus on a 3 MHz resonator.

in the vibrating part becomes rapidly less efficient with an, even slightly, non-vertical sidewall angle. For an angle around 3° which is reachable with the current process 1, Q_{anchor} fells down around 400 000 for the 3 MHz resonator as shown in Fig. 9 and 500 000 for the 2.2 MHz and explains the experimental values.

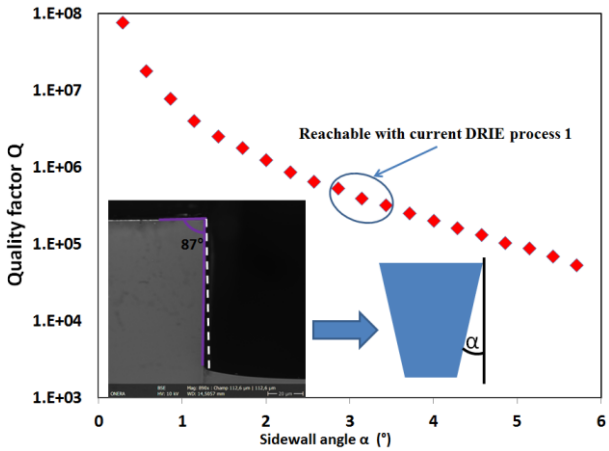

Fig. 9. Simulations using FEM of the Q_{anchor} vs sidewall angle for a 3 MHz type I resonator. In detail, scanning electron microscopy (SEM) of a 90 µm deep cross section beam.

B. Results of process 2

The craking with the process 2 was reduced but resonators shown lower performances as Q did not exceed 130 000 at 3 MHz and type II resonators showed better performances. The degraded quality factors are probably due the presence of the pyramids resulting from the wet etching of the cavities on the back side as illustrated in Fig 10. As there are no pyramids on the top face, the structure obtained with process 2 is less symmetrical than in the case of process 1, which may amplify the loss energy through the anchors and degrade Q_{anchor} hence the overall decrease of the experimental Q.

Table 2 shows the results of the different processes and designs used as well as previous work on resonators using the same mode of interest, R_m is the serie resistance in the standard BVD model.

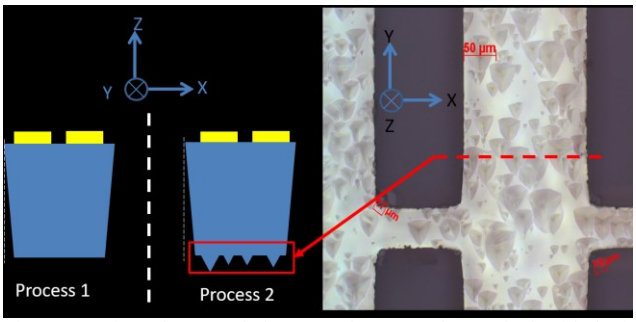

Fig. 10. Left: Schemes of the cross beam section etched with both processes. Right: photography of the back side of a resonator using wet etching and presence of pyramids with several tens of microns diameters.

Table 2: Experimental Q and Rm of the different types 2D-LEM obtained with the three process of the work and previous works on 2D-LEM.

Process	Design	f_{res} (MHz)	Q (10^3)	R_m (kOhms)	Q.f (10^{11} Hz)
1	I	2.2	135	7.8	3.0
		3.0	110	11	3.3
	II	2.2	180	5.4	4.0
		3.0	150	7.5	4.5
2	I	2.2	102	11	2.2
		3.0	98	11.3	2.9
		4.5	85	14.6	3.8
	II	3.0	129	8.5	3.9
		4.5	117	9.8	**5.3**
Dinger [3]		1.0	200	2.5	2.0
Kawashima [12]		1.5	350	0.28	5.2
		1.2	370	0.26	4.4
		1.1	430	0.31	4.7

One can note that the larger resonators (with lower resonant frequencies) present better performances than the smaller ones (higher resonant frequencies) and that was also observed in the work of Kawashima. Also, type II resonators have shown better perfomances than equivalent previous standard type I design which seems to indicate a more efficient design with the out of phase extension-compression mode of the lateral beams.

V. Conclusions

In this paper, new 2D-LEM quartz resonators with potential T&F applications have been demonstrated with first prototypes showing encouraging electro-mechanical characteristics providing a Q.f product near 10^{12} Hz. The two main limiting damping mecanisms have been identified: the energy loses arise on one hand from the the viscous dissipation in the gold layer forming the electrodes and on the other hand from the energy dissipation in the mounting areas. The latter one is amplified due to the slightly non vertical sidewall as well as from the surface rugosity induced the chemical wet etching of the cavities. Future work will be focused on improving the quality factor by tackling the aforementioned damping source.

Acknowledgment

This work is founded by the Centre National d'Etudes Spatiales CNES.

References

[1] O. Le Traon, M. Bahriz, O. Ducloux, S. Masson, and

D. Janiaud, “A Micro-Resonator for Fundamental Physics Experiments and its Possible Interest for Time and Frequency Applications,” *Jt. Conf. IEEE Int. Freq. Control Eur. Freq. Time Forum Proc.*, 2011.

[2] S. Ghaffari *et al.*, “Quantum limit of quality factor in silicon micro and nano mechanical resonators.,” *Sci. Rep.*, vol. 3, p. 3244, 2013.

[3] R. J. Dinger, “A minature quartz resonator vibrating at 1 MHz,” *Proc. 35 th Ann. Freq Control Symp.*, pp. 144–148, 1981.

[4] O. Le Traon, “Structure plane de résonateur mécanique découplé par des vibrations de flexion et d’extension compression,” n° 13/00322, 2013.

[5] O. Brand, I. Dufour, S. M. Heinrich, and F. Josse, *Resonant MEMS–Fundamentals, Implementation and Application*, First Edit. Wiley-VCH Verlag GmbH & Co. KGaA, 2015.

[6] B. Bourgeteau-verlhac, R. Lévy, T. Perrier, P. Lavenus, J. Guérard, and O. Le Traon, “Gold Thin Film Viscoelastic Losses of a Length Extension Mode Resonator,” *Eur. Freq. Time Forum*, pp. 1–4, 2016.

[7] R. Pelle, H. Christer, V. K. Ilia, and B. Ylva, “Etch rates of crystallographic planes in Z -cut quartz - experiments and simulation,” *J. Micromechanics Microengineering*, vol. 8, no. 1, p. 1, 1998.

[8] J. J. Boy, H. Tavernier, X. Vacheret, T. Laroche, and A. Clairet, “Collective fabrication of 20 MHz resonators by deep Reactive Ion Etching on 3" quartz wafers,” *Proc. IEEE Int. Freq. Control Symp. Expo.*, pp. 3–7, 2011.

[9] R. G. Nagele *et al.*, “A 995MHz Fundamental Nonlinear Quartz MEMS Oscillator,” pp. 566–570, 2013.

[10] A. Sankaran and M. J. Kushner, “Integrated feature scale modeling of plasma processing of porous and solid SiO2. I. Fluorocarbon etching,” *J. Vac. Sci. Technol. A Vacuum, Surfaces, Film.*, vol. 22, no. 4, p. 1242, 2004.

[11] H. Doh *et al.*, “Mechanism of selective SiO2 / Si etching with fluorocarbon gases (CF4 , C4F8) and hydrogen mixture in electron cyclotron resonance plasma etching system Mechanism of selective SiO 2 / Si etching with fluorocarbon gases (CF 4 , C 4 F 8) and hydrogen mixture in electron cyclotron resonance plasma etching system,” vol. 2827, no. 1996, 2014.

[12] H. Kawashima and M. Nakazato, “Variational analysis of new shape length extensional mode quartz crystal resonator taking account of lateral motion,” *Proc. 35 th Ann. Symp. Freq. Control*, pp. 378–386, 1981.